Kinetic analysis of antagonist action at N-methyl-D-aspartic acid receptors

Two binding sites each for glutamate and glycine

Morris Benveniste and Mark L. Mayer

Unit of Neurophysiology and Biophysics, Laboratory of Developmental Neurobiology, National Institute of Child Health and Human Development, National Institutes of Health, Bethesda, Maryland 20892 USA

ABSTRACT   Antagonism of glutamate-receptor responses activated by N-methyl-D-aspartic acid (NMDA) was studied using whole cell voltage clamp recording from mouse dissociated hippocampal neurons cultured for 10–15 d. The kinetics of onset of and recovery from NMDA receptor block during continuous application of NMDA together with either glycine, or L-alanine, were recorded in response to concentration jump application of NMDA- and glycine-binding site directed competitive antagonists, applied with a multibarrel flow pipe under conditions which allowed rapid solution changes around the cell < 10 ms. Mathematical solutions for both one- and two-equivalent site models for competitive antagonism were determined according to the differential equations outlined by Colquhoun and Hawkes (1977. *Proc. R. Soc. Lond. B.* 199:231–262). The kinetics of action of D-CPP and D-AP5, NMDA binding site antagonists, and 7Cl-kynurenic acid, a glycine binding site antagonist, were examined for each model. For all these antagonists, the kinetics for the onset of and recovery from antagonism were better fit by the two-equivalent site model, which yielded antagonist microscopic k_{Boff}/k_{Bon} values which closely approximated K_i values determined from analysis of equilibrium dose response curves. These results suggest that two molecules of NMDA and two molecules of glycine must bind to the NMDA receptor for activation of ion channel gating.

INTRODUCTION

Excitatory amino acid receptors in the mammalian central nervous system have been broadly divided into two major subtypes: N-methyl-D-aspartate (NMDA) and DL-α-amino-3-hydroxy-5-methyl-4-isoxazoleproprionic acid (AMPA)/kainate preferring receptors. Both subtypes can be activated by L-glutamate, and at many central synapses both NMDA and AMPA/kainate receptors contribute to the excitatory synaptic potential (Dale and Roberts, 1985; Huettner and Baughman, 1988; Forsythe and Westbrook, 1988). Characterizing the kinetics of ligand binding to these subtypes of the glutamate receptor family would enhance our understanding of the contribution each makes to synaptic mechanisms in vivo (e.g., Lester et al., 1990). In this paper, we analyze the kinetics of action of NMDA receptor antagonists using concentration jump techniques.

In equilibrium studies, with 3 μM glycine present continuously, excitatory amino acid potency for NMDA receptor activation varies over a 1,000-fold range, from an EC_{50} = 2.3 μM for L-glutamate to an EC_{50} = 2.3 mM for quinolinate (Verdoorn et al., 1989; Patneau and Mayer, 1990). For all agonists the Hill Coefficient, determined from a fit of the logistic equation to agonist activated currents, was > 1, indicating that more than

one NMDA agonist binding site on the receptor needs to be occupied for activation of ion channel gating; at low concentrations of NMDA the limiting slope of a double log plot of the dose response curve has a value near two (Patneau and Mayer, 1990).

At the molecular level, the activation of NMDA receptors is complicated by the fact that glycine appears to act as a co-agonist which is absolutely required for activation of ion channel gating (Johnson and Ascher, 1987; Kleckner and Dingledine, 1988; Vyklicky, et al., 1990), suggesting that both glutamate and glycine must occupy independent ligand binding sites before transitions to the open state can occur. Also, NMDA activated currents undergo desensitization, a component of which is sensitive to glycine concentration (Mayer et al., 1989; Lerma et al., 1990; Vyklicky et al., 1990). Recently, we have suggested that this glycine-sensitive desensitization results from the NMDA receptor existing in two states with different affinities for glycine (Benveniste et al., 1990a).

The analysis of dose response curves for the action of agonists does not always distinguish clearly between models with one, or more than one molecule of agonist required for activation of ion channel gating (e.g., Bean, 1990). One- and two-site models for receptor activation can be better distinguished by analysis of the kinetics of the response to concentration jump application of agonist, since a one-site model predicts an exponential activation time course, while two-site models predict

sigmoidal kinetics. However, with whole cell recording, high concentrations of agonist are required to yield large responses with a sufficient signal-to-noise ratio for kinetic analysis; with these conditions the rate of solution exchange and not the kinetics of agonist binding can become the limiting factor which determines the time course of receptor activation, unless, e.g., very rapid solution changes are achieved (Lester et al., 1990). This makes distinction between one- and two-site models difficult. Also, for both models, deactivation kinetics following removal of agonist are described by single exponential functions. In contrast to the rapid kinetics of action of agonists, the kinetics of onset of and recovery from block by the NMDA receptor competitive antagonists, i.e. 3-([±]-2-carboxypiperazin-4-yl)-propyl-1-phosphonic acid (D,L-CPP) and D-2-amino-5-phosphonopentanoic acid (D-AP5) (Olverman and Watkins, 1989) are relatively slow and less likely to be influenced by the rate of solution exchange (Benveniste et al., 1990b). Furthermore, the kinetics of both onset of and recovery from competitive antagonist block of agonist-activated responses are distinct for one and two binding site models. This is useful because analysis of the kinetics of agonist-activated responses during the rapid application of competitive *antagonists* can thus provide insight as to the number of *agonist* occupied sites required for activation of ion channel gating, in addition to providing useful information on antagonist binding kinetics.

In our previous experiments, antagonist association- and dissociation-rate constants (k_{Bon} and k_{Boff}, respectively) were determined by single exponential analysis of the response to concentration jump application of D-AP5 and D,L-CPP in the presence of 100 μM NMDA and 3 μM glycine (see Benveniste et al., 1990b), with a correction for receptor occupancy by agonist applied during analysis of the rate of onset of antagonist action ($1/\tau_{on}$) according to the equation:

$$\tau_{on} = \frac{1}{fk_{Bon}[B] + k_{Boff}}, \quad (1)$$

where

$$f = \frac{1}{1 + \frac{[A]}{EC_{50}}},$$

A and B represent agonist and antagonist, respectively, and EC_{50} is the dose of agonist which produces a half maximal response (Krouse et al., 1985). With this analysis, the estimates obtained for association and dissociation rate constants for D,L-CPP were good predictors of the antagonist equilibrium dissociation constant

(K_i) because the ratio k_{Boff}/k_{Bon} was only 1.5-fold different from the value determined from analysis of antagonist equilibrium dose-response curves fit with a single binding site isotherm. However, for D-AP5 and the glycine site directed NMDA receptor antagonist, 7Cl-kynurenic acid (Kemp et al., 1988), the ratio k_{Boff}/k_{Bon} differed 10.6-fold and 10.8-fold, respectively, from K_i values determined from equilibrium dose-response analysis (Benveniste et al., 1990b). The approximation of Eq. 1 is true only for conditions in which the kinetics of agonist binding and ion channel gating are much faster than those for the kinetics of antagonist binding, such that agonist and antagonist binding are always in equilibrium with the receptor during changes in the concentration of antagonist (Krouse et al., 1985). In the presence of 100 μM NMDA, the time constant for onset of block by 30 μM D-AP5 determined by single exponential analysis (31.1 ± 8.3 ms), was comparable to the time constant of decline in response to NMDA after rapid removal of agonist (27.2 ± 4.2 ms), indicating that the rates of channel closure and dissociation of agonist were likely to influence the rate of association of D-AP5 (Benveniste et al., 1990b), and thus invalidate the conditions required in Eq. 1.

In an attempt to obtain better correspondence between kinetic and equilibrium measurements for D-AP5 and 7Cl-kynurenic acid, we determined rate constants for antagonist binding from fits of analytically solved equations predicting receptor occupancy, and used one- and two-site models for analysis of antagonist equilibrium dose response curves as appropriate. We show here that the kinetics of antagonism for both the NMDA binding site antagonists D-CPP and D-AP5, as well as the glycine binding site antagonist 7Cl-kynurenic acid, are well fit by a model based on the assumption that the NMDA receptor has two binding sites each for glutamate and glycine.

MATERIALS AND METHODS

Culture conditions and electrophysiology

Neurons were cultured from a dissection of E16–E18 C57Bl/6 mouse hippocampi as previously described (Mayer et al., 1989), and plated on a glial feeder layer which has been cultured for 2–3 wk before the neuronal dissection. To create the feeder layer, P1 mouse hippocampi were dissected and plated at 125,000 cells per ml and grown in Eagles minimum essential medium (MEM) + 10% fetal calf serum. When the cell layer was confluent, the cultures were treated with fluorodeoxyuridine (55 μM, final concentration) to arrest cell division. Neurons were plated at 25–50,000 cells per ml and were maintained in MEM + 5% horse serum + an insulin-transferrin nutrient supplement (Guthrie et al., 1987). Experiments were generally performed 10–14 d after the neuronal plating.

Neurons were voltage clamped at −60 mV with an Axoclamp 2

amplifier (Axon Instruments) operating in the discontinuous mode at a switching frequency of ~10 kHz. Experiments were performed at room temperature (24–27°C). Extracellular solution consisted of (in millimolar): NaCl, 160; KCl, 2.5; CaCl$_2$, 2; MgCl$_2$, 1; glucose, 10; Hepes, 10; 10 μg/ml phenol red; and was titrated to pH 7.3 with NaOH and adjusted to 325 mOsm. 400 nM tetrodotoxin and 5 μM bicuculline methochloride were added to block action potential discharge and spontaneous inhibitory synaptic currents, respectively. The intracellular solution consisted of (in millimolar): CsMeSO$_3$, 125; CsCl, 15; CaCl$_2$, 0.5; MgCl$_2$, 3; CsBAPTA, 5; and MgATP, 2. The solution was titrated to pH 7.2 with CsOH and adjusted to 305 mOsm. Agonist and antagonist solutions were similar to control extracellular solution but contained only 0.2 mM Ca (to reduce desensitization) and were devoid of Mg (to prevent ion channel block). Intracellular calcium was strongly buffered with 5 mM BAPTA, to minimize activation of Ca-dependent ionic currents secondary to calcium influx through NMDA receptor channels. To further minimize the effects of desensitization, NMDA was applied at 10 μM, and glycine was present at 3 μM (Benveniste et al., 1990a; Vyklicky et al., 1990).

Rapid solution changes were made as previously detailed (Vyklicky et al., 1990). Briefly, a nine barrel flowpipe array (internal diam 356 μm per barrel) was positioned ~100 μm from the cell soma. A solution containing both agonist and antagonist was applied to the cell soma and surrounding dendrites. After the response to this solution reached equilibrium, a stepper motor moved the flowpipe array so that the adjacent barrel containing only agonist was positioned in front of the cell soma. A valve controller then simultaneously stopped the flow of the first solution and initiated the flow of the antagonist-free solution causing the cell to respond with an increase in inward current. After the new equilibrium response was reached, the stepper motor returned the flowpipe array to its original position. When this was achieved, application of the solution containing both agonist and antagonist commenced again; this resulted in a decrease in inward current, as antagonist block developed. Previously, we have shown that the time constant for solution exchange around the cell was ~10 ms or less (Vyklicky et al., 1990).

D-CPP was a gift of J. C. Watkins, University of Bristol, UK. D-AP5 and 7Cl-kynurenic acid were purchased from Tocris Neuramin (Buckhurst Hill, Essex, UK) and all other chemicals were from Sigma Chemical Co. (St. Louis, MO) or Fluka (Buchs, Switzerland).

Theory and analysis

The theory for the kinetics of receptor activation in response to agonist binding has already been described by Colquhoun and Hawkes (1977). The same theory can be applied to describe the kinetics of binding of a competitive antagonist in the presence of agonist. In deriving the equations for the action of agonists and antagonists, we have assumed that a receptor occupied by agonist is in rapid equilibrium with the open state of the channel, and we have not modeled the opening and closing transitions explicitly. A result of this simplification is that rate constants derived for binding and dissociation of agonist are apparent values, which reflect both agonist binding and ion channel gating kinetics. As presented in the Discussion, we believe that this simplification does not affect the accuracy of our analysis of experimental results with antagonists, and the values we present for antagonist association- and dissociation-rate constants should be close to their true values.

From Colquhoun and Hawkes (1977) we know that the differential equation:

$$\frac{d\mathbf{P}(t)}{dt} = \mathbf{P}(t)\mathbf{Q} \tag{2}$$

has the following solution which is a sum of exponential functions:

$$\mathbf{P}(t) = \mathbf{P}(0) \sum_{i=1}^{k} \mathbf{A}_i e^{\lambda_i t}, \tag{3}$$
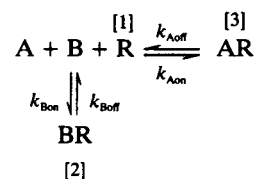
where $\mathbf{P}(t)$ is a vector composed of probabilities of the receptor occupying each of k states at time t, and $\mathbf{Q}$ is the matrix of transitions between the states described below. λ_i are the eigenvalues of $\mathbf{Q}$. $\mathbf{A}_i = m_i n_i$, where n_i denotes the ith row vector of matrix $\mathbf{N}$ and m_i denotes the ith column vector of matrix $\mathbf{M}$. $\mathbf{N}$ equals $\mathbf{M}^{-1}$ and $\mathbf{M}$ is composed of k column eigenvectors of $\mathbf{Q}$. Because $\mathbf{m}_i$ are eigenvectors of $\mathbf{Q}$, matrix $\mathbf{A}_i$ has special properties (Eq. 16 and 17 in Colquhoun and Hawkes, 1977) which allow the solution of $\mathbf{P}(t)$ to be written in the form of Eq. 3. $\mathbf{P}(0)$ represents a vector of initial probability of receptor state occupancies before the addition or removal of antagonists. In our experiments, we can only measure current flowing through open channels, which is correlated to the probability of the occupancy of the third receptor state, $\mathbf{P}_3(t)$, as defined in all of the following schemes. The fitting procedure can be streamlined by fitting only $\mathbf{P}_3(t)$ instead of the entire $\mathbf{P}(t)$ vector, using the solution:

$$\mathbf{P}_3(t) = \mathbf{P}(0) \sum_{i=1}^{k} \mathbf{A}_{i,3} e^{\lambda_i t}, \tag{4}$$

where $\mathbf{A}_{i,3}$ symbolizes the third column of matrix $\mathbf{A}_i$.

One binding site model

For a one-site model of competitive antagonism we can summarize agonist and antagonist binding reactions as:

$$
\begin{array}{c}
\qquad\qquad [1] \quad k_{Aoff} \quad [3] \\
A + B + R \underset{k_{Aon}}{\overset{}{\rightleftharpoons}} AR \\
k_{Bon} \big\updownarrow k_{Boff} \\
BR \\
[2]
\end{array}
$$

where [1], [2], and [3] represent the receptor, R, in the unbound, antagonist bound and agonist bound states, respectively, and A represents the agonist and B the competitive antagonist. The ion channel is assumed to be closed in states [1] and [2] and open in state [3]. The macroscopic transition matrix $\mathbf{Q}$ is composed of elements, q_{ij}, where the ith row represents the initial receptor state before the transition, and the jth column represents the final receptor state after the transition. The transition element, q_{ij}, for ligand association reactions is represented by the association-rate constant (k_{Aon} for agonist and k_{Bon} for antagonist) multiplied by ligand concentration, and for dissociation reactions q_{ij} is the concentration independent dissociation-rate constant (k_{Aoff} for agonist and k_{Boff} for antagonist). For the one-site model depicted above, the transition matrix is:

$$
\mathbf{Q} = \begin{bmatrix}
-(k_{Aon}[A] + k_{Bon}[B]) & k_{Bon}[B] & k_{Aon}[A] \\
k_{Boff} & -k_{Boff} & 0 \\
k_{Aoff} & 0 & -k_{Aoff}
\end{bmatrix}.
$$

The probability of occupancy of the receptor by agonist can be determined explicitly after diagonalizing $\mathbf{Q}$, by creating the $\mathbf{A}_i$ matrices

and solving Eq. 4. Then, the onset of current block after a rapid concentration jump application of antagonist is proportional to:

$$P_3(t) = \frac{q_{13}q_{21}}{\alpha\beta}$$

$$+ \frac{q_{13}q_{21} - \alpha(q_{13}P_1(0) + P_3(0)(q_{13} + q_{12} + q_{21})) + P_3(0)\alpha^2}{\alpha(\alpha - \beta)}e^{-\alpha t}$$

$$+ \frac{q_{13}q_{21} - \beta(q_{13}P_1(0) + P_3(0)(q_{13} + q_{12} + q_{21})) + P_3(0)\beta^2}{\beta(\beta - \alpha)}e^{-\beta t},$$

$$(5)$$

where

$$\alpha, \beta = \frac{-(q_{31} + q_{12} + q_{13} + q_{21})}{2}$$
$$\pm \frac{\sqrt{(q_{31} - q_{12} - q_{13} + q_{21})^2 + 4q_{12}q_{13}}}{2}.$$

After setting $k_{Bon}[B] = 0$ in matrix Q, recovery from antagonist block recorded after a concentration jump to antagonist-free solution, is proportional to:

$$P_3(t) = \frac{q_{13}}{q_{13} - q_{33}} - \frac{P_2(0)q_{13}}{q_{22} + q_{13} - q_{33}}e^{q_{22}t}$$

$$+ \left(P_3[0] - \frac{q_{13}}{q_{13} - q_{33}} + \frac{P_2(0)q_{13}}{q_{22} + q_{13} - q_{33}}\right)e^{(q_{33}-q_{13})t}. \quad (6)$$
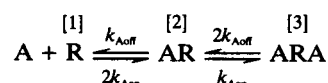
Eqs. 5 and 6 are the sum of 3 exponentials as predicted by Eq. 4, where the constant term $e^{\lambda t}$, when $\lambda = 0$, represents the time-independent steady-state level of occupancy for the activated state of the receptor. Analysis of the response to antagonist utilizing these equations was performed using fixed values for k_{Aon} and k_{Aoff}, the apparent rate constants for agonist association and dissociation according to a single binding site model. A single exponential was fit to the rise in current in response to agonist applied alone and k_{Aon} determined from a plot of $1/\tau_{on}$ vs. agonist concentration (Benveniste et al., 1990b). The exponential time constant, τ_{off}, was measured from the decline in the current trace in response to removal of agonist, and the agonist apparent microscopic dissociation-rate constant (k_{Aoff}) was determined as $1/\tau_{off}$.

The response to a concentration jump application of antagonist recorded with agonist present continuously contained two relaxations in our experimental protocol: the response to removal of antagonist, followed by the response to reapplication of antagonist; for all models these responses were analyzed together in pairs. First, the antagonist dissociation-rate constant, k_{Boff}, was determined iteratively, by fitting the time course of the increase in NMDA receptor current following step removal of antagonist to Eq. 6, and letting both the antagonist association-rate and dissociation-rate constants vary. Fitting of all the models was accomplished using a nonlinear Simplex fitting procedure (Kowalik and Osborne, 1968) which minimized the sum of the squared differences between the experimental data and the calculated current transient deduced from the sum of k exponentials according to Eq. 4. A unique solution for k_{Boff} determined for the one-site model could not be obtained without an additional constraint, thus the ratio of k_{Boff}/k_{Bon} was constrained to within three-fold of the K_i value determined from equilibrium dose response analysis. This constraint was not necessary

for any of the other fitting procedures described below. With k_{Boff} obtained from the previous fit now fixed, k_{Bon} for the one-site model was redetermined iteratively, by fitting the decline of NMDA receptor current recorded following the reapplication of antagonists to Eq. 5.

A two binding site model

Values for k_{Aon} and k_{Aoff}, the apparent microscopic rate constants for agonist association and dissociation were re-evaluated for a two-equivalent site model for agonist action by analysis of the response to concentration jump application of agonist. In this case, τ_{off} was obtained as described above, and k_{Aoff} determined as $1/2\tau_{off}$. The macroscopic transition matrix for the two equivalent site model for agonist action according to the scheme:
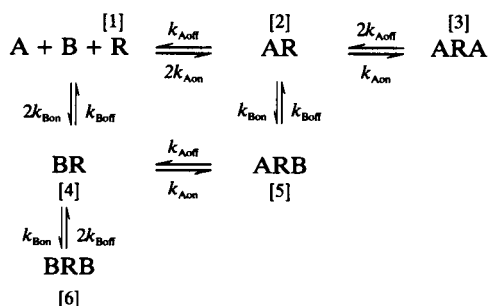
$$\overset{[1]}{A + R} \underset{2k_{Aon}}{\overset{k_{Aoff}}{\rightleftharpoons}} \overset{[2]}{AR} \underset{k_{Aon}}{\overset{2k_{Aoff}}{\rightleftharpoons}} \overset{[3]}{ARA}$$

is given by:

$$Q = \begin{bmatrix} -2k_{Aon}[A] & 2k_{Aon}[A] & 0 \\ k_{Aoff} & -(k_{Aon}[A] + k_{Aoff}) & k_{Aon}[A] \\ 0 & 2k_{Aoff} & -2k_{Aoff} \end{bmatrix}.$$

The coefficient of 2 in the matrix of macroscopic transitions from states [1] to [2] and from states [3] to [2] results from the summation of two microscopic transitions into and out of these states, with identical microscopic rate constants (Colquhoun and Ogden, 1988). After diagonalization of the above macroscopic transition matrix, the eigenvalues and eigenvectors can be incorporated into Eq. 4 yielding the explicit solution for the probability for occupancy of the activated state, ARA, of:

$$P_3(t) = \left(\frac{q_{23}}{q_{21} + q_{23}}\right)^2 + \left(\frac{q_{23}}{q_{21} + q_{23}}\right)^2 e^{-2(q_{21}+q_{23})t}$$

$$- 2\left(\frac{q_{23}}{q_{21} + q_{23}}\right)^2 e^{-(q_{21}+q_{23})t} \quad (7)$$

from which the agonist apparent microscopic association-rate constant (k_{Aon}) can be obtained iteratively.

The two-equivalent site model for competitive antagonism, in which state [3] is the activated receptor channel complex [ARA], can then be described as:

$$
\begin{array}{ccccc}
\overset{[1]}{A + B + R} & \underset{2k_{Aon}}{\overset{k_{Aoff}}{\rightleftharpoons}} & \overset{[2]}{AR} & \underset{k_{Aon}}{\overset{2k_{Aoff}}{\rightleftharpoons}} & \overset{[3]}{ARA} \\
2k_{Bon} \updownarrow k_{Boff} & & k_{Bon} \updownarrow k_{Boff} & & \\
BR & \underset{k_{Aon}}{\overset{k_{Aoff}}{\rightleftharpoons}} & ARB & & \\
{[4]} & & {[5]} & & \\
k_{Bon} \updownarrow 2k_{Boff} & & & & \\
BRB & & & & \\
{[6]} & & & &
\end{array}
$$

where the transition matrix is:

$$Q = \begin{bmatrix} -2(k_{Aon}[A] + k_{Bon}[B]) & 2\,k_{Aon}[A] & 0 & 2\,k_{Bon}[B] & 0 & 0 \\ k_{Aoff} & -(k_{Bon}[B] + k_{Aoff} + k_{Aon}[A]) & k_{Aon}[A] & 0 & k_{Bon}[B] & 0 \\ 0 & 2\,k_{Aoff} & -2\,k_{Aoff} & 0 & 0 & 0 \\ k_{Boff} & 0 & 0 & -(k_{Aon}[A] + k_{Bon}[B] + k_{Boff}) & k_{Aon}[A] & k_{Bon}[B] \\ 0 & k_{Boff} & 0 & k_{Aoff} & -(k_{Aoff} + k_{Boff}) & 0 \\ 0 & 0 & 0 & 2\,k_{Boff} & 0 & -2\,k_{Boff} \end{bmatrix}$$

In contrast to the above cases, this two-site analysis for the onset of and recovery from antagonist evoked block could not be solved explicitly in terms of k_{Bon} and k_{Boff}. This results from the fact that a model with six receptor states has a 6 × 6 transition matrix Q which would yield a sixth order polynomial that cannot be solved analytically to determine the eigenvalues. Thus, the eigenvalues were determined by numerical approximation using IMSL routines. In this analysis, values for k_{Aon} and k_{Aoff} were previously determined for the two-site model for agonist action as described above, and held constant during the determination of the antagonist microscopic rate constants. In each iteration, k_{Bon} and k_{Boff} were modified and eigenvalues and eigenvectors of Q determined. First, k_{Boff} was determined by fitting the kinetics of the response to removal of the antagonist, where the antagonist association- and dissociation-rate constants were the freely variable parameters in the Simplex fit. Although $k_{Bon}[B]$ was set equal to 0 in the transition matrix for the fit of recovery from antagonist block, its value had to be determined for the estimation of the values in the $P(0)$ vector. The calculated current transient is proportional to the sum of six exponentials according to Eq. 4. At this point, the ratio k_{Boff}/k_{Bon} determined solely from the fit of recovery from antagonist block was usually within two- to threefold of the K_i determined from equilibrium dose response analysis. After k_{Boff} was determined, its value was fixed and k_{Bon} became the only variable rate constant used in fitting the response to reapplication of antagonist later in the same current trace. Because each of the models detailed above describes receptor occupancy and not membrane current, an additional variable proportional to the number of receptors and the single channel current had to be included to convert receptor occupancy into a whole cell current response.

In the figures, the solid lines represent either a one- or two-site analysis fit as appropriate. The range over which the solid line is drawn represents the range of points over which the data was fit. Simulated current transients were constructed by a numerical methods approach as detailed elsewhere (Benveniste et al., 1990a).

Selection of analysis procedure

Analysis using one- and two-equivalent site models for NMDA receptor block by competitive antagonists yielded better fits when the kinetics of the response to antagonist removal were analyzed first to determine k_{Boff}, and then the kinetics of the response to reapplication of antagonist were analyzed second to determine k_{Bon}, using a fixed value for k_{Boff} in the transition matrix. Curves were less well fit when k_{Boff} and k_{Bon} were determined simultaneously by analyzing the responses to antagonist removal and reapplication in one fit. By fitting the onset of, and recovery from antagonism simultaneously, estimated values for k_{Bon} and k_{Boff} would be weighted equally for both phases of the concentration jump response, although the time course of the response to removal of antagonist contains no information pertaining to the antagonist association-rate constant except for the initial amplitude ($P(0)$). Thus, by fitting the response to removal of and reapplication of antagonist separately, the analysis is likely to weight the data more appropriately than in the case of a simultaneous fit.

RESULTS

Kinetic analysis of agonist-induced currents

The analysis of NMDA receptor responses during onset of and recovery from antagonism according to the analytically determined equations for the models described in Materials and Methods requires prior analysis of the response to agonist applied alone, since the apparent rate constants for binding and dissociation of *agonist* are held as fixed parameters during analysis of *antagonist* responses. Although previous work suggests that a single-site model for activation of NMDA receptors is unlikely to be valid (Patneau and Mayer, 1990; Benveniste et al., 1990a), we determined k_{Aon} and k_{Aoff} for both one- and two-site models for agonist action to be able to check the validity of one- and two-site models for antagonist action. These experiments were performed in the presence of 3 μM glycine. Within the limited temporal resolution of our concentration jump experiments, responses to NMDA were reasonably well fit by both one- and two-site models for agonist action. For the two-site model for agonist action the apparent association rate constant for NMDA (k_{Aon}), 2.08 ± 0.9 μM^{-1}s^{-1} (7 cells, 66 observations), was calculated iteratively utilizing Eq. 7; for the one-site model k_{Aon} was determined as 1.12 μM^{-1}s^{-1} from the slope of the plot of $1/\tau_{on}$, estimated by single exponential analysis of the response to application of NMDA (Benveniste et al., 1990b). The apparent microscopic dissociation-rate constant for NMDA (k_{Aoff}) for the two-site analysis was determined from single exponential fits to the decrease in membrane current after removal of agonist, and is half of the value (i.e., ½τ_{off}) calculated for a single binding site model. Values for k_{Aoff} were determined to be 45.72 ± 7.37 s^{-1} and 22.86 ± 3.69 s^{-1} for one- and two-site models, respectively. The ratio k_{Aoff}/k_{Aon} for the two-site model, 11.0 μM, is in reasonable agreement with the microscopic K_d of 16.4 μM determined from a two-equivalent site analysis of the NMDA equilibrium dose response curve (Patneau and Mayer, 1990). An example of a

response to NMDA fit by two-site analysis is shown in Fig. 1.

For the glycine site of the NMDA receptor, the kinetics of the response to concentration jump application of both the high affinity agonist glycine, and the low-affinity agonist L-alanine, were also analyzed using both one- and two-site models for agonist action. Glycine concentration jumps were performed in the presence of 10 μM NMDA. Two-site analysis gave estimates for k_{Aon} and k_{Aoff} of 13.61 ± 0.9 $\mu M^{-1}s^{-1}$ and 1.00 ± 0.13 s^{-1}, respectively (6 cells, 50 observations). Single exponential analysis of the response to concentration jump
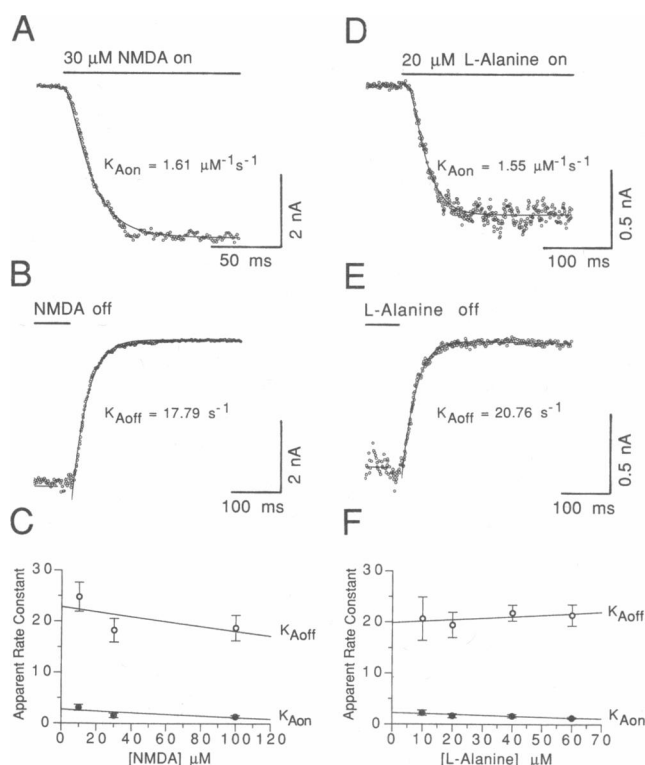

FIGURE 1   Kinetic analysis of the action of NMDA and L-alanine according to a two-equivalent binding site model; solid lines indicate the fit of a two-site model for agonist action. A and B are portions of a continuous record of membrane current recorded in the presence of 3 μM glycine during a concentration jump of 30 μM NMDA. Analysis of trace B gave $\tau_{off} = 28.1$ ms, corresponding to a $k_{Aoff} = 17.79$ s^{-1}. Eq. 7 was used for analysis of the trace shown in A, yielding a $k_{Aon} = 1.61$ $\mu M^{-1}s^{-1}$. C shows that for NMDA mean values for k_{Aon} (2.1 $\mu M^{-1}s^{-1}$) and k_{Aoff} (23 s^{-1}) vary slightly with agonist concentration. D and E are portions of a continuous record of membrane current recorded in the presence 100 μM NMDA during a concentration jump of 20 μM L-alanine. Analysis of trace D gave $\tau_{off} = 24.08$ ms, corresponding to a $k_{Aoff} = 20.76$ s^{-1}. Eq. 7 was used for analysis of the trace shown in E, yielding a $k_{Aon} = 1.55$ $\mu M^{-1}s^{-1}$. F shows that for L-alanine k_{Aon} (1.7 $\mu M^{-1}s^{-1}$) and k_{Aoff} (19.9 s^{-1}) do not vary appreciably with concentration. Solid lines in C and F represent fits to the data by linear regression analysis.

application of glycine with a one binding site model yielded average estimates for $k_{Aon} = 10.4$ $\mu M^{-1}s^{-1}$ and $k_{Aoff} = 2.00 \pm 0.25$ s^{-1}. These values were similar to those previously reported for glycine applications in the presence of 100 μM NMDA (Benveniste et al., 1990b).

For responses to L-alanine recorded in the presence of 100 μM NMDA values for k_{Aon} and k_{Aoff} determined by two-site analysis were 1.73 ± 0.51 $\mu M^{-1}s^{-1}$ and 19.88 ± 2.87 s^{-1}, respectively (6 cells, 96 observations). The average values for k_{Aon} and k_{Aoff} for the one-site model were 0.89 $\mu M^{-1}s^{-1}$ and 39.76 ± 5.74 s^{-1}. An example of two-site kinetic analysis of the response to a concentration jump application of 20 μM L-alanine is illustrated in Figs. 1, D and E. The ratio k_{Aoff}/k_{Aon} for the two-site model has a value of 11.5 μM, similar to the microscopic K_d of 15.3 μM determined from analysis of the L-alanine equilibrium dose response curve by a two-equivalent site model (data not shown).

Kinetic analysis of inhibition of NMDA induced currents by D-CPP and D-AP5

Although both one- and two-site models for agonist action gave reasonable fits to concentration jump responses evoked by NMDA, for the response to NMDA receptor *antagonists* much better fits were obtained with the two-site model. Fig. 2 shows examples of the change in membrane current recorded from hippocampal neurons exposed to 10 μM NMDA and 3 μM glycine, during application of and removal of D-CPP and D-AP5. Compared with our previous work (Benveniste et al., 1990b), the kinetics of onset of block by D-AP5 were slightly faster in the present experiments, consistent with reduction of the concentration of NMDA from 100–10 μM, and a competitive interaction between D-AP5 and NMDA.

Two-site analysis of the response to 1.5 and 6 μM D-CPP, which dissociates slowly in comparison to NMDA (10 μM), yielded mean values for k_{Bon} and k_{Boff} of 3.6 ± 1.4 $\mu M^{-1}s^{-1}$ and 1.1 ± 0.1 s^{-1} (5 cells, 45 observations), respectively. These values were within 1.5-fold of the values previously determined by single exponential analysis and the correction factor given by Eq. 1 (Benveniste et al., 1990b). For one-site analysis we obtained mean values of 3.9 ± 1.4 $\mu M^{-1}s^{-1}$ for k_{Bon} and 0.5 ± 0.1 s^{-1} for k_{Boff}, but as illustrated in Figs. 2, A and B, fits of the one-site model were not good. Two-site analysis of the response to 11 and 15 μM D-AP5 in the presence of 10 μM NMDA and 20 μM D-AP5 in the presence of 30 μM NMDA, yielded mean values for k_{Bon} and k_{Boff} of 22.23 ± 6.5 $\mu M^{-1}s^{-1}$ and 19.45 ± 4.1 s^{-1} (7 cells, 48 observations), respectively. D-AP5, which dissociates rapidly compared with D-CPP, has mean value for k_{Bon} that is 14.8 times
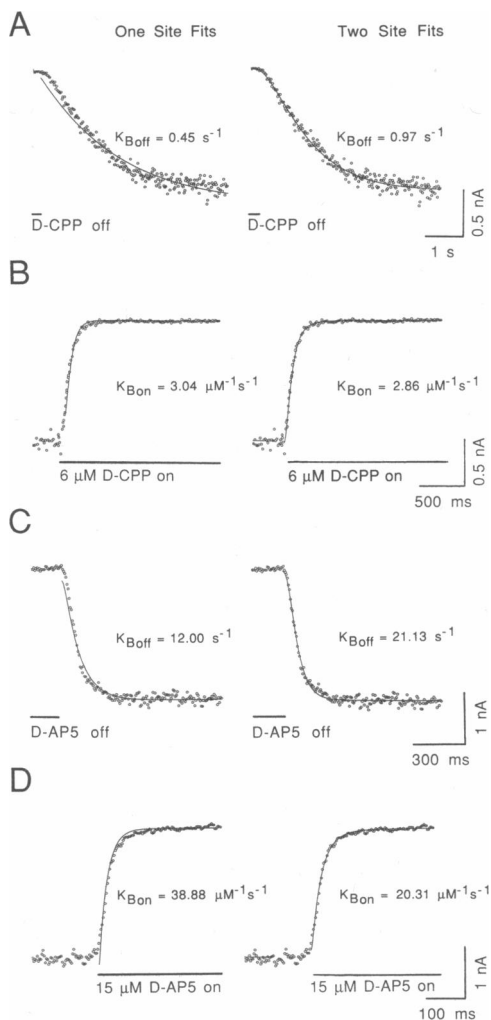
FIGURE 2 Kinetic analysis of the action of D-CPP and D-AP5 fit with one- and two-equivalent site models for competitive antagonism. Each antagonist was applied by concentration jump in the presence of 10 μM NMDA and 3 μM glycine, with the responses to removal of, and reapplication of antagonist displayed separately. Traces A and C show digitized records of membrane current recorded during the removal of 6 μM D-CPP (A) or 15 μM D-AP5 (C). Traces B and D show the onset of antagonism during the reapplication of 6 μM D-CPP (B) or 15 μM D-AP5 (D). Solid lines in the left column indicate nonlinear least squares fits to a one binding site model for antagonist action used to determine the antagonist dissociation-rate constant (A and C) from Eq. 6, or the antagonist association-rate constant (B and D) from Eq. 5. Solid lines in the right column represent nonlinear least squares fits to a two binding site model for antagonist action as detailed in Materials and Methods. For the one binding site analysis (left column), the apparent rate constants for agonist binding were: k_{Aon} = 1.12 μM^{-1}s^{-1}; k_{Aoff} = 45.71 s^{-1}; for the two equivalent site analysis (right column), apparent rate constants for agonist action were: k_{Aon} = 2.08 μM^{-1}s^{-1}; k_{Aoff} = 22.86 s^{-1}.

greater than that determined by single exponential analysis, while the mean k_{Boff} values are similar (Table 1 and Benveniste et al., 1990b). For one-site analysis we obtained mean values of 48.8 $\pm$ 22.5 μM^{-1}s^{-1} for k_{Bon} and 12.1 $\pm$ 3.0 s^{-1} for k_{Boff}; as noted for D-CPP, fits of the one-site model to responses evoked by D-AP5 were not good.

The goodness of fit of the one-site model (determined from the residual sum of squared errors after curve fitting with the Simplex algorithm) was heavily dependent on the starting point chosen for the analysis, and on the concentration of antagonist used. The goodness of fit of the two-equivalent site model was less sensitive to the starting point chosen for the analysis. In some cases, responses to removal of and reapplication of antagonists were better fit by a one-site model for antagonist action than the examples shown in Fig. 2, but k_{Boff}/k_{Bon} ratios calculated from these responses were several-fold different from K_i values estimated using a single binding site model to analyze equilibrium dose response curves for antagonist action, consistent with errors in the estimation of either antagonist rate constants or the equilibrium value for K_i with single site models.

Our kinetic analysis for D-CPP and D-AP5 gave clearly distinguishable fits for one- and two-site models (Fig. 2). The better fit of the two-site model is consistent with both equilibrium analysis of dose response curves for activation of NMDA receptors (Patneau and Mayer, 1990), and with analysis of the kinetics of desensitization at NMDA receptors (Benveniste et al., 1990a) which both suggest two binding sites for NMDA. The simulated response of a two-site model for antagonist action, when fit with the one-site model used for analysis of responses to D-CPP and D-AP5, showed striking similarities between the poor fit of the one-site model to experimental data, and the poor fit of the one-site model to data simulated by the two-site model (compare Figs. 2 and 3). To understand the significance of an inadequate fit for our models of antagonist action, it is important to realize that the degree of block at equilibrium, and the kinetics of onset of and recovery from block are not independent variables which can be freely adjusted to obtain the best fit. Instead, the kinetics of antagonist action are determined by k_{Bon} and k_{Boff}, while the ratio of these values determines antagonist potency ($K_i = k_{Boff}/k_{Bon}$). The one-site model underestimates the degree of block at equilibrium both before removal of antagonist (Fig. 3 A), and following reapplication of antagonist (Fig. 3 B). The response to removal of antagonist predicted by the one-site model does not reach steady state as fast as either the response simulated by the two-site model (Fig. 3 A), or experimental data recorded with D-CPP and D-AP5 (Fig. 2). In contrast, the onset of antagonism predicted by the one-site model reaches
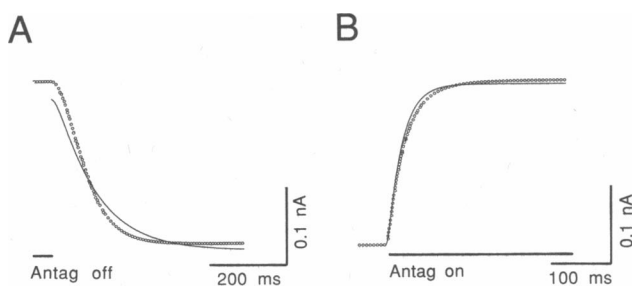
FIGURE 3 Analysis of two-site simulated responses by a one-site model. The response to a concentration jump application of antagonist was simulated by a two-site model for antagonist action (*small circles*) and analyzed using a one-site model for antagonist action (*solid line*). *A* shows recovery from antagonism, *B* the onset of antagonism. Values for agonist and antagonist binding kinetics were chosen such that they approximated the experimental values obtained with NMDA and D-AP5. Parameters for two-site model simulation were: $k_{Aon} = 2$ $\mu M^{-1}s^{-1}$, $k_{Aoff} = 23\ s^{-1}$, $k_{Bon} = 16\ \mu M^{-1}s^{-1}$, $k_{Boff} = 20\ s^{-1}$, $[A] = 10\ \mu M$ agonist, $[B] = 10\ \mu M$ antagonist. To determine k_{Aon} and k_{Aoff} for the one-site model analysis, the response of the two-site model to agonist concentration jumps was simulated (not shown), and the results fit with single exponential functions. Agonist and antagonist association and dissociation rate constants obtained by one-site analysis of these simulated responses were: $k_{Aon} = 1.2\ \mu M^{-1}s^{-1}$, $k_{Aoff} = 46\ s^{-1}$, $k_{Bon} = 20.5$ $\mu M^{-1}s^{-1}$, $k_{Boff} = 9.9\ s^{-1}$.

steady state faster than the response simulated by the two-site model for antagonist action (Fig. 3 *B*); a similar discrepancy occurs for experimentally recorded responses to D-CPP and D-AP5 (Fig. 2).

The simulations shown in Fig. 3 were generated by a two binding site model for antagonist action with association and dissociation rate constants similar to those found experimentally for D-AP5 and NMDA, and illustrate the response to instantaneous step application of and removal of antagonist. The sigmoidal kinetics of the response to removal of D-AP5 and D-CPP (Fig. 2) is thus revealed in Fig. 3 *A* to be a consequence of agonist and antagonist binding kinetics, and not the kinetics of solution exchange. The results of this simulation give added confidence to our suggestion that a one-site model for antagonism cannot accurately fit the kinetics of responses to concentration jump application of competitive NMDA receptor antagonists, but do provide support for the two-site model as a satisfactory alternative.

Comparison between equilibrium and kinetic measurements for competitive antagonists

Although the one-site model for competitive antagonism poorly fit the time course of the response to concentration jump application of D-CPP and D-AP5, the corre-spondence between K_i values for D-CPP and D-AP5 calculated from analysis of antagonist equilibrium dose-response curves using a single binding site model, with K_i values calculated from the ratio k_{Boff}/k_{Bon} also derived using a single binding site model, was much better than when single exponential analysis was used to analyze the kinetics of antagonist responses (cf. Benveniste et al., 1990b). This is because the single binding site model for antagonist action does not require the assumption of rapid re-equilibration of agonist and antagonist binding during a concentration jump application of antagonist to receptors pre-equilibrated with agonist (see Eq. 1). From single site analysis, the ratio k_{Boff}/k_{Bon} determined for D-CPP was $0.15 \pm 0.06\ \mu M$, which is 1.5-fold less than the K_i value determined from analysis of the equilibrium inhibition of NMDA activated currents by D-CPP fit using a single binding site isotherm. However, for the fast dissociating antagonist D-AP5 the ratio k_{Boff}/k_{Bon} determined by the one-site model for antagonist action, $0.29 \pm 0.12\ \mu M$, is still fourfold less than the K_i value determined from analysis of antagonist dose response curves using a single binding site isotherm. For these experiments, equilibrium dose-response analysis was performed for five concentrations of D-CPP or D-AP5 in the presence of 10 μM NMDA and 3 μM glycine (Fig. 4, *A* and *B*).

For two-site analysis of the response to D-CPP, the ratio k_{Boff}/k_{Bon} yields a microscopic K_i of $0.37 \pm 0.16\ \mu M$ which is in excellent agreement with the equilibrium microscopic K_i of $0.40 \pm 0.02\ \mu M$ determined from analysis of antagonist dose response curves according to the equation for equilibrium block using a two-site model:

$$\% \text{ of Control} = \frac{100}{\left(1 + \dfrac{[B]}{K_o}\right)^2}, \tag{8}$$

where K_o represents the concentration at which the number of binding sites occupied by agonist is reduced by 0.5 at any fixed value of agonist concentration [A]. An example of the dose-response curve for D-CPP fit with this model is shown in Fig. 4 *C*. The antagonist microscopic equilibrium dissociation constant, K_i, is then determined from the Cheng-Prusoff equation (Cheng and Prusoff, 1973):

$$K_i = \frac{K_o}{1 + \dfrac{[A]}{K_d}}, \tag{9}$$

where K_d is the apparent microscopic equilibrium dissociation constant for binding of agonist, determined using a two binding site model. For this analysis the microscopic K_d for NMDA, 11.0 μM, was calculated from the
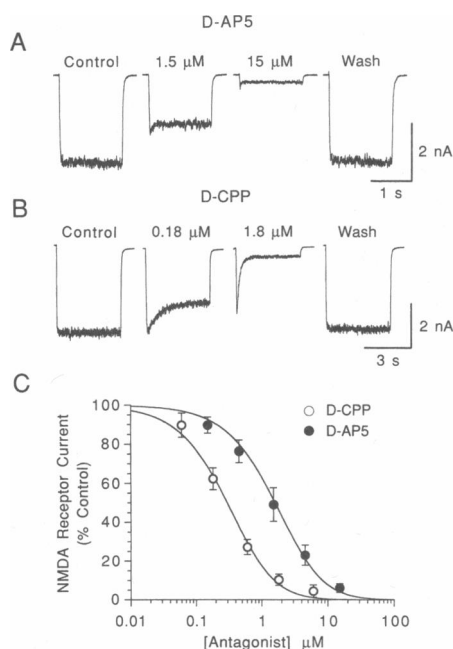
FIGURE 4 Equilibrium dose-response data for competitive NMDA receptor antagonists analyzed with a two binding site model. A shows responses to concentration jump application of 10 μM NMDA, applied together with the indicated concentrations of D-AP5; 3 μM glycine was present continuously. The activation of NMDA receptors by agonist and the onset of antagonism by D-AP5 reach equilibrium with similar kinetics. B shows similar responses, in a different neuron, for D-CPP. Initially, the response to NMDA overshoots its equilibrium value, because the onset of antagonism by D-CPP is slow to reach equilibrium. C shows the equilibrium dose response curve for block of the response to NMDA by D-AP5 and D-CPP; data points are the mean $\pm$ S.D. of values recorded from four neurons per antagonist. The solid line drawn through the data points was obtained by a least squares fit of Eq. 8, the equilibrium equation for a two binding site model.

ratio k_{Aoff}/k_{Aon} determined by two-site analysis as described above. Simulations of antagonist responses were used to confirm that the determination of K_i from Eqs. 8 and 9 is valid for a two binding site model. For D-AP5 the ratio k_{Boff}/k_{Bon} = 0.92 $\pm$ 0.23 μM, also in good agreement with the microscopic K_i for D-AP5 of 1.93 $\pm$ 0.28 μM determined from equilibrium dose response analysis with a two-equivalent binding site model.

Kinetic analysis of inhibition of NMDA induced currents by 7Cl-kynurenic acid

Dose response analysis of equilibrium responses to glycine at a constant concentration of NMDA have yielded Hill coefficients ranging from 0.77 to 1.44 (Kleckner and Dingledine, 1988; Lerma et al., 1990; Vyklicky et al., 1990). Thus there is some uncertainty as to the

number of glycine binding sites on the NMDA receptor which need to be occupied for activation of ion channel gating. By performing kinetic analysis for the response to an NMDA receptor glycine site competitive antagonist, analogous to the analysis performed for NMDA receptor glutamate site competitive antagonists and described above, we hoped to determine the stoichiometry of glycine binding sites for activation of the NMDA receptor channel complex.

The antagonist used, 7Cl-kynurenic acid, is a high affinity, competitive, glycine-site directed NMDA receptor antagonist, with only low affinity for the NMDA binding site (Kemp et al., 1988). In order for the on-response to application of competitive antagonists to be fit properly by either one- or two-site models, we have observed empirically that the data from concentration jump experiments must show a decrease in the time constant for onset of antagonism with increasing concentration of antagonist. Previously, we have shown by single exponential analysis that such a relationship does not exist for the block of NMDA receptor responses by 7Cl-kynurenic acid in the presence of glycine (Benveniste et al., 1990b, see also Henderson et al., 1990). However, when L-alanine was substituted for glycine, the time constant for onset of antagonism by 7Cl-kynurenic acid did become faster as the concentration of antagonist was increased. The apparent microscopic dissociation-rate constant for L-alanine is 20 times faster than that for glycine (see above). Thus, we concluded that the kinetics of dissociation of glycine were rate limiting when compared with the association rate for binding of 7Cl-kynurenic acid to the NMDA receptor, causing concentration-independent kinetics for the antagonist action of 7Cl-kynurenic acid. Consistent with this, an off response to removal of agonist, of similar kinetics to, or faster than the response to onset of antagonist action, also was the minimal requirement for two-site analysis, otherwise a unique solution to the fitting procedure was not attainable. When 100 μM L-alanine was used instead of 3 μM glycine to promote activation of NMDA receptors, our data for the antagonist action of 7Cl-kynurenic acid could be fit by both one- and two-site binding models, but as described below, fits were better with the two-site model.

The upper traces of Figs. 5, A and B show typical results for fits of the onset of and recovery from NMDA receptor antagonism evoked by 10 μM 7Cl-kynurenic acid in the presence of 100 μM NMDA and 100 μM L-alanine according to a one-site model for antagonism (Eqs. 5 and 6). Note that the apparent association- and dissociation-rate constants for the agonist (L-alanine) were determined by prior single exponential analysis as described earlier. Again, the poor fit obtained is qualitatively similar to those for the action of the competitive
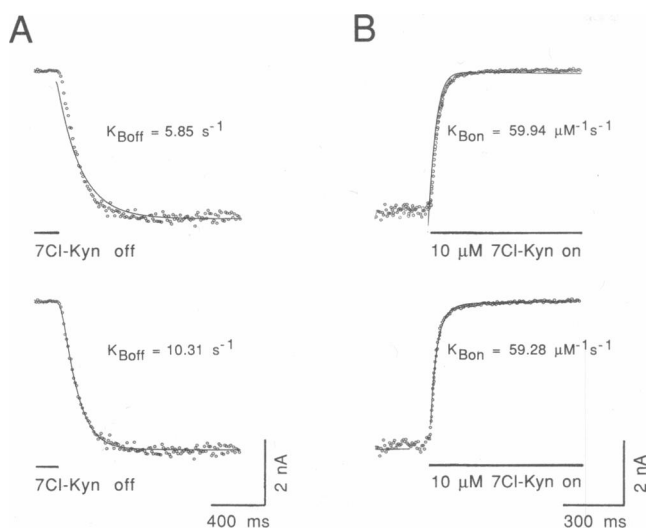
FIGURE 5 Kinetic analysis of the action of 7Cl-kynurenic acid according to one- and two-binding site models. Traces show digitized records of membrane currents recorded in the presence of 100 μM NMDA and 100 μM L-alanine during the removal of 10 μM 7Cl-kynurenic acid (A), or its reapplication (B). Upper traces indicate data fit to a one binding site model from which the antagonist dissociation-rate constant (A) or association-rate constant (B) was determined. Agonist kinetics for the one binding site model were: $k_{Aon} = 0.89$ μM^{-1}s^{-1}, $k_{Aoff} = 39.76$ s^{-1}. Lower traces indicate the same data fit to a two binding site model from which the antagonist microscopic dissociation-rate constant (A) or microscopic association-rate constant (B) were determined. Agonist kinetics for the two binding site model were: $k_{Aon} = 1.73$ μM^{-1}s^{-1}, $k_{Aoff} = 19.88$ s^{-1}.

NMDA antagonists D-CPP and D-AP5 shown in Fig. 2 and for the simulated response of a two-site model for competitive antagonism shown in Fig. 3. Analysis of responses to the removal and reapplication of 10 and 30 μM 7Cl-kynurenic acid in the presence of 100 μM L-alanine, yielded a mean k_{Boff} value derived by analysis using the one-site model of 6.2 ± 0.3 s^{-1} and a mean k_{Bon} of 31.1 ± 9.4 μM^{-1}s^{-1}. This yielded a k_{Boff}/k_{Bon} ratio of 0.22 ± 0.08 μM which is similar to the previously determined steady state K_i (Benveniste et al., 1990b; Vyklicky et al., 1990); however, this value has little meaning because the curves were not well fit (Fig. 5).

In the lower traces of Figs. 5, A and B, the kinetics of action of 7Cl-kynurenic acid were reanalyzed for the same experimental traces, but using the two-site model. The onset of and recovery from antagonism are now well fit. The average k_{Bon} for 7Cl-kynurenic acid was 40.77 ± 14.8 μM^{-1}s^{-1} and the average k_{Boff} was 10.68 ± 0.5 s^{-1} (6 cells, 24 observations). The microscopic K_i determined from the ratio k_{Boff}/k_{Bon} for the action of 7Cl-kynurenic acid in the presence of L-alanine is 0.30 ± 0.10 μM. This value is in good agreement with the value of 0.14 μM, obtained from an independent determination of K_i by a

two-site model analysis of the dose response curve for equilibrium block of responses to 100 μM NMDA and 3 μM glycine by 7Cl-kynurenic acid. For the latter analysis $K_o = 5.7$ μM, and the microscopic K_d used in Eq. 9 was 73 nM. This was determined from the ratio of k_{Aoff}/k_{Aon} from kinetic analysis utilizing a two site model of glycine concentration jumps (see above). These K_i values for 7Cl-kynurenic acid are also good agreement with measurements from binding experiments (Kemp et al., 1988).

DISCUSSION

We have demonstrated that kinetic analysis of concentration jump data recorded with NMDA receptor competitive *antagonists* can be used to differentiate between one and two site models for activation of ion channel gating by the *agonists* NMDA and L-alanine. For each of the three antagonists studied, comparison of K_i values determined from the ratio of k_{Boff}/k_{Bon} with K_i values determined from analysis of equilibrium dose response curves, indicates that kinetic analysis utilizing either one- or two-site models yielded better estimates of rate constants for antagonist binding than exponential analysis (Table 1). However, the goodness of fit to the time course of antagonist action was much better for the two site model. It should be noted that the two-site model used for antagonist action does *not* require binding of two molecules of antagonist for block of ion channel activity; rather, binding of a single molecule of antagonist to either of a pair of identical agonist recognition sites is sufficient to block activation of the receptor.

Kinetic analysis of the action of D-AP5 and D-CPP confirms results from equilibrium dose-response analysis with low concentrations of NMDA which indicated that two molecules of agonist must bind to the NMDA receptor for activation of ion channel gating (Patneau and Mayer, 1990). However, in previous experiments using equilibrium measurements, the stoichiometry of activation of the NMDA receptor by glycine could not be accurately assessed because the contamination of experimental solutions by nanomolar concentrations of endogenous glycine made it impossible to determine the limiting slope of the glycine log–log dose response curve. The kinetic experiments with 7Cl-kynurenic acid described here overcame this difficulty because they were performed with high doses of the glycine-like agonist, L-alanine (100 μM), and thus contamination by nanomolar concentrations of endogenous glycine is insignificant. Our results clearly indicate the existence of a stoichiometry of two for binding of glycine to the NMDA receptor on hippocampal neurons. This is consistent with recent biochemical analyses (Thedinga et al., 1989; Yeh et al.,

	k_{Bon}	k_{Boff}	k_{Boff}/k_{Bon}	K_i
	$\mu M^{-1}s^{-1}$	s^{-1}	μM	μM
D-AP5				
Exponential Analysis	1.5	19.6	13.3	1.23
One Site Analysis	48.8 ± 22.5	12.1 ± 3.0	0.29 ± 0.12	1.09
Two Site Analysis	22.2 ± 6.5	19.4 ± 4.1	0.92 ± 0.23	1.93
D-CPP				
Exponential Analysis	1.9*	1.4	0.7	0.23*
One Site Analysis	3.9 ± 1.4	0.5 ± 0.1	0.15 ± 0.06	0.22
Two Site Analysis	3.6 ± 1.4	1.1 ± 0.1	0.37 ± 0.16	0.40
7Cl-Kynurenic Acid				
Exponential Analysis	3.0	8.5	2.8	0.26
One Site Analysis	31.1 ± 9.4	6.2 ± 0.3	0.22 ± 0.08	0.14
Two Site Analysis	40.8 ± 14.8	10.7 ± 0.5	0.30 ± 0.10	0.14

Note the unusually slow binding kinetics for D-CPP. K_i values were determined from equilibrium dose response analysis using one or two binding site isotherms. The ratio k_{Boff}/k_{Bon} is in good agreement K_i values for one- and two-site analysis but not for exponential analysis. Errors are given as standard deviations. For exponential analysis (data from Benveniste et al., 1990b) * indicates that a racemic mixture of CPP was used and that the k_{Bon} value was multiplied by two, and the K_i value divided by two because only one optical isomer of CPP is a potent NMDA receptor antagonist (Aebischer et al., 1989).

1990) and the results of our analysis of the kinetics of desensitization at NMDA receptors (Benveniste et al., 1990a). In Table 1, the rate constants for D-AP5, D-CPP, and 7Cl-kynurenic acid obtained from one- and two-equivalent binding site analysis are compared with those previously determined by single exponential analysis (Benveniste et al., 1990b).

The kinetic analysis of our data made several important assumptions, concerning the influence of ion channel gating on the kinetics of action of antagonists, the effects of noninstantaneous solution changes, and the existence of agonist and antagonist binding sites of equivalent affinity for two-site models. These points are discussed below.

Influence of ion channel opening and closing rate constants on antagonist responses

The models described in Materials and Methods represent a simplified subset of one- and two-site models because the additional steps of ion channel opening and closing were omitted (e.g., Cachelin and Colquhoun, 1989). As a result, our values for agonist microscopic association- and dissociation-rate constants will be in error; however, as described below, the effect of this on the calculation of microscopic association- and dissociation-rate constants for antagonists is surprisingly small. Simulations were performed for concentration jump application of antagonists in which the two-equivalent site model used for analysis of our experimental data

was used to fit simulated data generated by a two-site model containing an extra transition, between a closed state with two molecules of agonist bound and the open state, with a ratio of opening to closing rate constants of β/α. To generate the simulated data sets α and β were varied while the agonist and antagonist association- and dissociation-rate constants were kept constant. The simulated responses were then analyzed using the two-site kinetic analysis program, in which the opening and closing transitions were neglected. The apparent association- and dissociation-rate constants determined from this analysis (in which opening and closing kinetics were ignored) were then compared with the original simulated values.

To simulate responses similar to those evoked by the fast dissociating antagonist D-AP5, values for k_{Bon} and k_{Boff} were set at 16 $\mu M^{-1}s^{-1}$ and 20 s^{-1}, while k_{Aon} and k_{Aoff} were simulated as 2 $\mu M^{-1}s^{-1}$ and 23 s^{-1}, respectively, to give responses similar to those evoked by NMDA. When α was simulated at $\alpha \geq 200$ s^{-1} with $\beta \geq 0.1$, fits of the two-site model to antagonist concentration jump responses were good at all concentrations of agonist and antagonist. With values of $\alpha \leq 30$ s^{-1}, k_{Bon} was variable and changed with antagonist concentration. As a result, our model implies that there will be many openings per burst. Single channel measurements of NMDA receptor activity, with mean open times between 2.5 and 7 ms, yield experimental values for α close to or greater than the 200 s^{-1} required for accurate analysis of antagonist kinetics (Nowak et al., 1984; Ascher et al., 1988; Jahr and Stevens, 1987; Howe et al., 1988; Cull-Candy and

Usowicz, 1989; Jahr and Stevens, 1990). The analysis of single channel data is less informative concerning values for β because closed time constants within bursts determined from multi-exponential fits ranged from 7 μs to 250 ms (Howe et al., 1988; Cull-Candy and Usowicz, 1989). In our simulations, with values for $\alpha \geq 200$ s^{-1}, a 100-fold variation in β from 10 to 1,000 s^{-1} produced less than twofold variation in k_{Bon} and k_{Boff} estimated from our 2-site analysis program in which transitions to the open state were not explicitly modeled.

Effects of noninstantaneous concentration jumps on antagonist responses

The models described in Materials and Methods also assumed instantaneous applications of agonist and antagonist. Analysis of data with this assumption is capable of producing valid results in the case of noninstantaneous solution changes, if the time course for agonist and antagonist action is slower than the time required for a solution change in the vicinity of the cell. Previously, we have estimated the solution exchange time constant by bathing cells in 50 μM kainate with 5 mM external sodium and measuring the time course of the rise in current recorded on jumping into a solution containing 165 mM external sodium (Vyklicky et al., 1990). The time constant of this process was <10 ms. With subsequent improvements to our system, and by choosing neurons without extended processes, we can routinely measure kinetics with exponential time constants of 7 ms.

We have conducted simulations to test the effect of a noninstantaneous solution exchange on our analysis of association and dissociation rates for agonists and antagonists. The parameters for simulation of agonist and antagonist kinetics were the same as described in the previous section. With a solution exchange time constant of 5 ms the average value for k_{Aon} determined by kinetic analysis assuming a two-site model was 1.6 μM^{-1}s^{-1}, 20% lower than the parameter used in the simulation. The mean value determined for k_{Aoff}, 20.1 s^{-1}, was 12.5% lower than the parameter used for simulation. However, for analysis of simulated responses to applications of antagonists, at concentrations similar to those used in our experiments, the value estimated for k_{Boff} did not vary significantly from the parameter used for simulation, while k_{Bon} increased only 8%. Even with a solution exchange time constant of 10 ms, k_{Boff} still did not vary significantly from the simulation parameter of 20 s^{-1} while k_{Bon} increased <27%. The fact that the ratio of k_{Boff}/k_{Bon} for each antagonist tested was similar to its respective K_i determined from equilibrium dose response analysis also indicates that the effect of noninstan-

taneous concentration changes is not a major concern for the ligands examined in the present experiments. For slowly dissociating antagonists, like D-CPP, the effects of noninstantaneous solution changes are inconsequential.

A different problem arises when the rate of onset of block by high concentrations of antagonist becomes limited by the time course of agonist dissociation, even though the antagonist is applied with a fast solution change. Using the above values for k_{Aon}, k_{Aoff}, k_{Bon}, and k_{Boff}, analysis of simulated responses to application of 30 μM antagonist (which produced >99% inhibition), did not yield a unique solution for k_{Bon}, even though accurate fits were obtained at lower concentrations of antagonist. To avoid this complication, it is important to obtain estimates for the kinetics of antagonist action over a range of antagonist concentrations.

Models with nonequivalent binding sites

A two-site model for competitive antagonism contains 12 microscopic transitions. If all the transitions were not equivalent, then 24 rate constants would need to be determined; however, when the two-sites are of equivalent affinity the number of rate constants is reduced to 4. Although a two equivalent site model was used in the present analysis, agonist-preferring and antagonist-preferring states have been proposed on the basis of autoradiographic studies (Monaghan et al., 1988). Also, we have suggested that the NMDA receptor can exist in states with high and low affinity for NMDA, and high and low affinity for glycine (Benveniste et al., 1990a). The change in affinity for NMDA does not appear to be dependent on excitatory amino acid binding site occupancy as in the cases of normal positive and negative cooperativity, but depends on occupancy by glycine of its binding sites. Similarly, this model proposes the analogous situation for glycine binding, namely: glycine affinities change with occupancy of the binding sites for NMDA. A two-equivalent site model for the NMDA/ AP5-CPP binding site can be used as a reasonable approximation, provided that the glycine concentration is kept high enough so that binding sites for NMDA will exist in only one of the different affinity states. The concentrations used for our experiments, 3 μM glycine and 100 μM L-alanine, are near the top of their dose-response curves. The same argument holds for measuring kinetics at the glycine site: NMDA concentrations should either be low or high to force the receptor into a single state for binding glycine.

D-CPP yielded an average k_{Bon} of 2.4 μM^{-1}s^{-1} at 6 μM and 4.7 μM^{-1}s^{-1} at 1.5 μM. Although k_{Boff} did not vary significantly over the same range, the approximate twofold change in k_{Bon} with a fourfold change in antago-

nist concentration was characteristic of all the antagonists tested. The variability in k_{Bon} recorded in our experiments could result from the oversimplification of our model as a result of not including explicit channel opening and closing transitions, as discussed above, or by the NMDA receptor having two nonequivalent agonist binding sites, with fits constrained to a two equivalent site model during our analysis. These simplifications may also explain the slight deviation of agonist apparent association and dissociation rate constants with concentration. Also, responses to low concentrations of agonist or antagonist were less well fit, most likely because the poor signal-to-noise ratio does not provide enough information for accurate kinetic analysis.

Comparison of glutamate and glycine binding sites

Conformationally restricted competitive antagonists developed from phosphonic amino acid derivatives appear to have unusually slow binding kinetics at the excitatory amino acid recognition site on the NMDA receptor complex. When experiments are performed under identical conditions, the glutamate recognition site on the NMDA receptor behaves quite differently with respect to conformationally restricted antagonists for both the glycine binding site on the NMDA receptor, and the excitatory amino acid binding site on the AMPA/kainate receptor. For NMDA receptors the association-rate constant for 7Cl-kynurenic acid, a conformationally restricted glycine site antagonist, is 11 times faster than that for the NMDA binding site antagonist D-CPP. The antagonist action of quinoxaline 6-cyano-7-nitroquinoxaline-2,3-dione (CNQX), which is a potent, selective non-NMDA receptor antagonist (Honoré et al., 1988) with considerable conformational restriction, also has faster kinetics of action than D-CPP. Recovery from CNQX-evoked block of responses to kainic acid occurs rapidly (for a two binding site analysis the dissociation-rate constant for CNQX is ≈ 23 s^{-1}, i.e., 21 times faster than that for D-CPP; Benveniste and Mayer, unpublished observations). Because the potency of antagonist action of CNQX on AMPA/kainate receptors is similar to that of D-CPP on NMDA receptors, this implies that the association-rate constant for binding of CNQX to AMPA/kainate receptors must also be much faster than that for binding of D-CPP to NMDA receptors, despite the fact that CNQX is a more constrained molecule than D-CPP.

Based on a comparison between CPP, CNQX, and 7Cl-kynurenic acid, the limited data available from our experiments suggests that conformational restriction of competitive antagonists for glutamate receptors does not as a rule produce ligands with slow association

kinetics. It is plausible that the excitatory amino acid antagonist binding site on NMDA receptors has molecular features, such as a pocket of restricted accessibility, which reduces the probability that molecules of CPP colliding with their binding site will be in the correct orientation for a successful interaction with the receptor. Another possibility is that phosphonate antagonists have unusual chemical or kinetic properties. Currently, we are using the techniques described here in conjunction with a large series of competitive antagonists to examine structural features which are responsible for determining antagonist binding kinetics at the NMDA receptor.

REFERENCES

Aebischer, B., P. Frey, H. P. Haerter, P. Herrling, W. Mueller, H. J. Olverman, and J. C. Watkins. 1989. Synthesis and NMDA antagonistic properties of the enantiomers of 4-(3-phosphonopropyl)piperazine-2-carboxylic acid (CPP) and of the unsaturated analogue (E)-4-(3-phosphonoprop-2-enyl)piperazine-2-carboxylic acid (CPP-ene). *Helv. Chim. Acta.* 72:1043–1051.

Ascher, P., P. Bregestovski, and L. Nowak. 1988. N-methyl-D-aspartate activated channels of mouse central neurones in magnesium free solutions. *J. Physiol. (Lond.).* 399:247–266.

Bean, B. 1990. ATP-activated channels in Rat and Bullfrog sensory neurons: concentration dependence and kinetics. *J. Neurosci.* 10:1–10.

Benveniste, M., J. Clements, L. Vyklicky Jr., and M. L. Mayer. 1990a. A kinetic analysis of the modulation of N-Methyl-D-Aspartic acid receptors by glycine in cultured mouse hippocampal neurones. *J. Physiol. (Lond.).* 428:333–357.

Benveniste, M., J. M. Mienville, E. Sernagor, and M. L. Mayer. 1990b. Concentration jump experiments with NMDA antagonists in mouse cultured hippocampal neurons. *J. Neurophys.* 63:1373–1384.

Cachelin, A. B., and D. Colquhoun. 1989. Desensitization of the acetylcholine receptor of frog end-plates measured in a vaseline-gap voltage clamp. *J. Physiol. (Lond.).* 415:159–188.

Cheng, Y. C., and W. H. Prusoff. 1973. Relationship between the inhibition constant (K_i) and the concentration of inhibitor which causes 50 per cent inhibition (I_{50}) of an enzymatic reaction. *Biochem. Pharmacol.* 22:3099–3108.

Colquhoun, D., and A. G. Hawkes. 1977. Relaxation and fluctuations of membrane currents that flow through drug-operated channels. *Proc. R. Soc. Lond. B.* 199:231–262.

Colquhoun, D., and D. C. Ogden. 1988. Activation of ion channels in the frog end-plate by high concentrations of acetylcholine. *J. Physiol. (Lond.).* 395:131–159.

Cull-Candy, S. G., and M. M. Usowicz. 1989. On the multiple-conductance single channels activated by excitatory amino acids in large cerebellar neurones of the rat. *J. Physiol. (Lond.).* 415:555–582.

Dale, N., and A. Roberts. 1985. Dual-component amino acid-mediated synaptic potentials: excitatory drive for swimming in *Xenopus* embryos. *J. Physiol. (Lond.).* 363:35–59.

Forsythe, I. D., and G. L. Westbrook. 1988. Slow excitatory postsynaptic currents mediated by N-methyl-D-aspartate receptors on cultured mouse central neurones. *J. Physiol. (Lond.).* 396:515–533.

Guthrie, P. B., D. E. Brenneman, and E. A. Neale. 1987. Morphological and biochemical differences expressed in separate dissociated cell cultures of dorsal and ventral halves of the mouse spinal cord. *Brain Res.* 420:313–323.

Henderson, G., J. W. Johnson, and P. Ascher. 1990. Competitive antagonists and partial agonists at the glycine modulatory site of the mouse N-methyl-D-aspartate receptor. *J. Physiol. (Lond.).* 430:189–212.

Honoré, T., S. N. Davies, J. Drejer, E. J. Fletcher, P. Jacobsen, D. Lodge, and F. E. Nielsen. 1988. Quinoxalinediones: potent competitive non-NMDA glutamate receptor antagonists. *Science (Wash. DC.).* 241:701–703.

Howe, J. R., D. Colquhoun, and S. G. Cull-Candy. 1988. On the kinetics of large-conductance glutamate-receptor ion channels in rat cerebellar granule neurones. *Proc. R. Soc. Lond. B.* 233:407–422.

Huettner, J. E., and R. W. Baughman. 1988. The pharmacology of synapses formed by identified corticocollicular neurons in primary cultures of rat visual cortex. *J. Neurosci.* 8:160–175.

Jahr, C. E., and C. F. Stevens. 1987. Glutamate activates multiple single channel conductances in hippocampal neurons. *Nature (Lond.).* 325:522–525.

Jahr, C., and C. F. Stevens. 1990. A quantitative description of NMDA receptor-channel kinetic behavior. *J. Neurosci.* 10:1830–1837.

Johnson, J. W., and P. Ascher. 1987. Glycine potentiates the NMDA response of mouse central neurones. *Nature (Lond.).* 325:529–531.

Kemp, J. A., A. C. Foster, P. D. Leeson, T. Priestley, R. Tridgett, L. L. Iverson, and G. N. Woodruff. 1988. 7-Chlorokynurenic acid is a selective antagonist at the glycine modulatory site of the N-methyl-D-aspartate receptor complex. *Proc. Natl. Acad. Sci. USA.* 85:6547–6550.

Kleckner, N. W., and R. Dingledine. 1988. Requirement for glycine in activation of NMDA-receptors expressed in *Xenopus* oocytes. *Science (Wash. DC.).* 241:835–837.

Kowalik, J., and M. R. Osborne. 1968. Methods for Unconstrained Optimization Problems. Elsevier, New York.

Krouse, M. E., H. A. Lester, N. H. Wassermann, and B. F. Erlanger. 1985. Rates and equilibria for a photoisomerizable antagonist at the acetylcholine receptor of *Electrophorus* electroplaques. *J. Gen. Physiol.* 86:235–256.

Lerma, J., R. S. Zukin, and M. V. L. Bennett. 1990. Glycine decreases desensitization of n-methyl-D-aspartate (NMDA) receptors expressed in *Xenopus* oocytes and is required for NMDA responses. *Proc. Natl. Acad. Sci. USA.* 87:2354–2358.

Lester, R. A. J., J. D. Clements, G. L. Westbrook, and C. E. Jahr. 1990. Channel kinetics determine the time course of NMDA receptor-mediated synaptic currents. *Nature (Lond.).* 346:565–567.

Mayer, M. L., L. Vyklicky Jr., and J. Clements. 1989. Regulation of NMDA receptor desensitization in mouse hippocampal neurons by glycine. *Nature (Lond.).* 338:425–427.

McBain, C. J., N. W. Kleckner, S. Wyrick, and R. Dingledine. 1990. Structural requirements for activation of the glycine coagonist site of NMDA receptors expressed in Xenpus oocytes. *Mol. Pharmacol.* 36:556–565.

Monaghan, D. T., H. J. Olverman, L. Nguyen, J. C. Watkins, and C. W. Cotman. 1988. Two classes of N-methyl-D-aspartate recognition sites: differential distribution and differential and differential regulation by glycine. *Proc. Natl. Acad. Sci. USA.* 85:9836–9840.

Nowak, L., P. Bregestovski, P. Ascher, A. Herbet, and A. Prochiantz. 1984. Magnesium gates glutamate-activated channels in mouse central neurons. *Nature (Lond.).* 307:462–465.

Olverman, H. J., and J. C. Watkins. 1989. NMDA agonists and competitive antagonists. *In* The NMDA receptor. J. C. Watkins and G. L. Collingridge, editors. Oxford University Press, Oxford. 19–36.

Patneau, D. K., and M. L. Mayer. 1990. Structure-activity relationships for amino acid transmitter candidates acting at N-methyl-D-aspartate and quisqualate receptors. *J. Neurosci.* 10:2385–2399.

Thedinga, K. H., M. S. Benedict, and G. E. Fagg. 1989. The N-Methyl-D-Aspartic acid (NMDA) receptor complex: a stoichiometric analysis of radioligand binding domains. *Neurosci. Lett.* 104:217–222.

Verdoorn, T. A., N. W. Kleckner, and R. Dingledine. 1989. N-methyl-D-aspartate/glycine and quisqualate/kainate receptors expressed in Xenopus oocytes: antagonist pharmacology. *Mol. Pharmacol.* 35:360–368.

Vyklicky Jr., L., M. Benveniste, and M. L. Mayer. 1990. Modulation of N-Methyl-D-Aspartic acid receptor desensitization by glycine in cultured mouse hippocampal neurones. *J. Physiol. (Lond.).* 428:313–331.

Yeh, G. C., D. W. Bonhaus, and J. O. McNamara. 1990. Evidence that zinc inhibits N-methyl-D-aspartate receptor-gated ion channel activation by noncompetitive antagonism of glycine binding. *Mol. Pharmacol.* 38:14–19.